Phase separation in a homogeneous shear flow: Morphology, growth laws, and dynamic scaling

Ludovic Berthier
Laboratoire de Physique, École Normale Supérieure, 46 Allée d'Italie, F-69007 Lyon, France
and Département de Physique des Matériaux, UCB Lyon 1, 43 Boulevard du 11 Novembre 1918,
69622 Villeurbanne Cedex, France
(Received 18 November 2000; published 11 April 2001)

We numerically investigate the influence of a homogeneous shear flow on the spinodal decomposition of a binary mixture by solving the Cahn-Hilliard equation in a two-dimensional geometry. Several aspects of this much studied problem are clarified. Our numerical data show unambiguously that, in the shear flow, the domains have on average an elliptic shape. The time evolution of the three parameters describing this ellipse is obtained for a wide range of shear rates. For the lowest shear rates investigated, we find the growth laws for the two principal axis $R_\perp(t) \sim$ const, $R_\parallel(t) \sim t$, while the mean orientation of the domains with respect to the flow is inversely proportional to the strain. This implies that when hydrodynamics is neglected, a shear flow does not stop the domain growth process. We also investigate the possibility of dynamic scaling, and show that only a nontrivial form of scaling holds, as predicted by a recent analytical approach to the case of a nonconserved order parameter. We show that a simple physical argument may account for these results.

DOI: 10.1103/PhysRevE.63.051503 PACS number(s): 05.70.Ln, 47.55.Kf, 64.75.+g

I. INTRODUCTION

The study of phase ordering kinetics has a long history [1–3]. The canonical example is the coarsening process following the quench of a binary mixture A-B below its spinodal line. The properties of the resulting domain growth are rather well understood [1–3]. In the case where A and B are in equal concentrations, an isotropic bicontinuous structure emerges, which is characterized by a typical length scale $L(t)$ growing as a power law of time t. Moreover, as t increases, the structure evolves in a self-similar manner in the sense that its statistical properties are the same when space is rescaled by $L(t)$. Any function $C(\mathbf{r},t)$ that depends on space and time is then a function of the reduced variable $|\mathbf{r}|/L(t)$ only: $C(\mathbf{r},t) \equiv \mathcal{C}(|\mathbf{r}|/L(t))$. This property is termed ''dynamic scaling'' [1–3].

The study of the spinodal decomposition in a homogeneous shear flow is of fundamental and practical interest [4], but despite an enormous amount of experimental [5–11], numerical [12–23], and analytical works [4,12,24–26], the problem is still not fully settled [26]. Early experiments [5,6,11] and simulations [19,20,23] showed that isotropy is lost, the morphology of the bicontinuous structure being elongated along the flow direction. Hence a single length scale cannot describe the full structure. There are thus several questions which naturally arise. (1) How to characterize quantitatively the growing structure? (2) What is the time dependence of the different length scales, as compared to the unsheared case? (3) Does the growth stop after some time? (4) Does a suitable generalization of the dynamic scaling property hold?

It is interesting to remark that in spite of the large number of works cited above, definite answers to all these questions are still lacking. Several reasons make this problem nontrivial. First, the role of hydrodynamics is far from being understood. Simple physical arguments [4] show that it may become preponderant at large times, predicting a saturation of the domains at a typical size. This assumption is resolved neither at the experimental level (see, e.g., the opposite conclusions of Refs. [7] and [11]) nor at the numerical level, where powerful algorithms are needed to deal with hydrodynamics correctly. At present, this limits the numerical analysis to sizes too small to make any definite answers to questions (1)–(4) above, although much progress was made recently [13–16].

Second, at the theoretical level, no analytical solution of a reasonable model of spinodal decomposition (even neglecting hydrodynamics) is available. One then has to make some predictions from the solution of solvable, but less realistic models, like the $O(n)$ model in the large-n limit [24], or from the approximate solution in the case of a nonconserved order parameter [25]. A scaling argument, based on the hypothesis that a generalization of dynamic scaling holds, was developed in Ref. [12].

Third, there are, to our knowledge, no numerical simulations (neglecting hydrodynamics) validating these analytical predictions. Moreover, the scaling hypothesis on which the analytical argument of Ref. [12] is based was only tested in Ref. [9], with negative results. Thus the validity of the predicted growth laws may also be questioned. More crucially, up to now there has been no consensus concerning the numerically measured growth laws: we discuss this point in a more detailed way in Sec. VI.

In this work, we numerically study the spinodal decomposition process in a shear flow by solving the Cahn-Hilliard equation in two dimensions. All hydrodynamic effects are neglected. Although this involves a drastic reduction of the experimental situation, it is necessary, in our opinion, to have a good understanding of this ''simple'' case before studying more realistic problems. Our algorithm is different, but our study is technically comparable to the most recent one [12]. However, we shall explore a wider range of shear rates, and this will lead us to a different interpretation of the numerical data.

The paper is organized as follows. In Sec. II, we define the model and describe the numerical procedure to solve it.

Section III briefly recalls the results obtained when the shear flow is absent. Section IV describes the morphology of the domains under shear and its time evolution. Section V focuses on the problem of dynamic scaling. In Sec. VI, we compare our results with the relevant existing data in the literature, and give a simple physical argument to explain them.

II. MODEL AND DETAILS OF THE SIMULATION

In this work we focus on the standard model for the spinodal decomposition of binary mixtures, and numerically solve the Cahn-Hilliard equation [1–4]

$$\frac{\partial \phi(\mathbf{r},t)}{\partial t}+\mathbf{v}\cdot\boldsymbol{\nabla}\phi(\mathbf{r},t)=\Gamma\nabla^2\left(\frac{\delta F[\phi]}{\delta\phi(\mathbf{r},t)}\right)+\eta(\mathbf{r},t). \quad (1)$$

In this expression, the order parameter $\phi(\mathbf{r},t)$ is a scalar quantity which can be linked to the concentration c_A (c_B) of the component A (B) of the mixture by the relation $\phi\equiv 1-2c_A=2c_B-1$. Equation (1) has the form of a continuity equation, which implies that the order parameter is a conserved quantity. The free energy $F[\phi]$ is of Ginzburg-Landau type,

$$F[\phi]=\int d^d\mathbf{r}\left[\frac{\xi^2}{2}|\boldsymbol{\nabla}\phi|^2+\frac{1}{4}\phi^4-\frac{1}{2}\phi^2\right], \quad (2)$$

where the equilibrium correlation length ξ is introduced. The noise term η is a random Gaussian variable, characterized by the two moments $\langle\eta(\mathbf{r},t)\rangle=0$ and $\langle\eta(\mathbf{r},t)\eta(\mathbf{r}',t')\rangle=-2T\delta(t-t')\nabla^2\delta(\mathbf{r}-\mathbf{r}')$; T is the temperature of the thermal bath. All the simulations will be carried out at $T=0$, since temperature is essentially irrelevant in this process [3] (it is also known to delay the onset of the asymptotic regime [27]). The second term on the left-hand side of Eq. (1) results from the advection of the order parameter by the velocity field. The case of a homogeneously sheared system will be investigated. The flow is taken to be in the x direction, and the velocity field is then $\mathbf{v}=\gamma y\mathbf{e_x}$, which defines the shear rate γ. We shall concentrate on the case of a constant shear rate.

We want then to solve the following equation numerically in two spatial dimensions:

$$\frac{\partial\phi}{\partial t}=-\gamma y\frac{\partial\phi}{\partial x}-\Gamma\nabla^2(\xi^2\nabla^2\phi-\phi^3+\phi), \quad (3)$$

where both space and time dependences have been removed for clarity. This is done by combining the numerical methods of Refs. [28,29]. A new frame (x',y') is first defined by [28] $x'\equiv x-S(t)y$, $y'\equiv y$, where $S(t)\equiv\int_0^t dt'\,\gamma$ is the strain. In the case of a constant shear rate, it is simply given by $S(t)=\gamma t$. Further defining $\phi(\mathbf{r},t)\equiv\hat{\phi}(\mathbf{r}',t)$, Eq. (3) becomes [28]

$$\frac{\partial\hat{\phi}(\mathbf{r},t)}{\partial t}=-\hat{\nabla}^2(\hat{\nabla}^2\hat{\phi}-\hat{\phi}^3+\hat{\phi}), \quad (4)$$

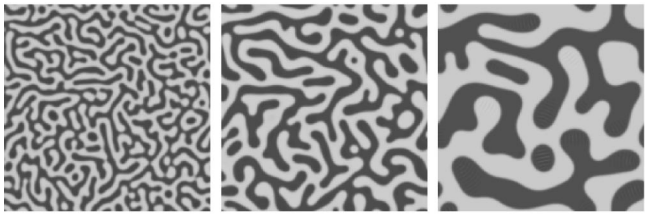

FIG. 1. Snapshots of size 256×256 of the unsheared spinodal decomposition at times $t=70$, 381, and 3761 (from left to right). Each color represents one phase of the mixture.

with

$$\hat{\boldsymbol{\nabla}}=\left(\frac{\partial}{\partial x'},\frac{\partial}{\partial y'}-S(t)\frac{\partial}{\partial x'}\right),$$

$$\hat{\nabla}^2=\left(\frac{\partial}{\partial x'}\right)^2+\left(\frac{\partial}{\partial y'}-S(t)\frac{\partial}{\partial x'}\right)^2. \quad (5)$$

After transformation, Eq. (4) is formally identical to the Cahn-Hilliard equation without shear, which is solved by the implicit spectral algorithm developed in Ref. [29]. Space is measured in units of the correlation length ξ (also the interface width) and time in units of ξ^2/Γ. This microscopic time scale represents the typical time it takes to create a well-defined domain wall. Periodic boundary conditions are imposed on the deformed frame. The single parameter of the simulation is then the shear rate γ, which introduces a time scale γ^{-1}. The choice of parameters for the discretization was discussed in Ref. [29], and the values $\Delta t=0.5$, $\Delta x=\Delta y=0.5$ are used throughout the simulation. For each shear rate, the system size has been carefully checked to be large enough so that the reported growth laws are unaffected by the boundaries. Since the growth is strongly anisotropic, a rectangular simulation box has been chosen with sizes up to $L_y=512$ and $L_x=8192$. The shear rates investigated in this paper are $\gamma=0.04$, 0.02, 0.01, 0.005, 0.0025, and 0.00125. This corresponds to a time scale γ^{-1} in the range [25,800]. We wish to emphasize that the condition $\gamma^{-1}\gg\xi^2/\Gamma$ has to be fulfilled, since we are interested in a scaling regime where well-defined domains coarsen. This remark will become important for the interpretation of the numerical results. An alternative solution would be to apply the shear flow after an

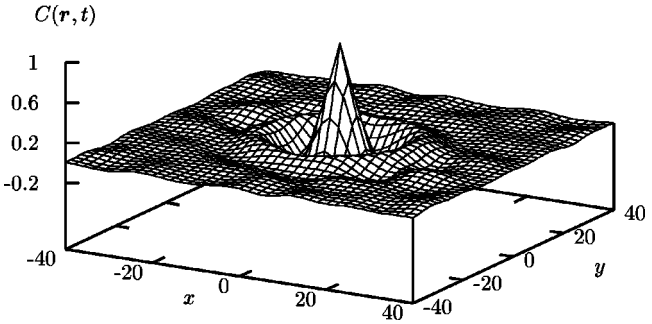

FIG. 2. Two-point correlation function [Eq. (6)], in the $\gamma=0$ case, at time $t=100$.

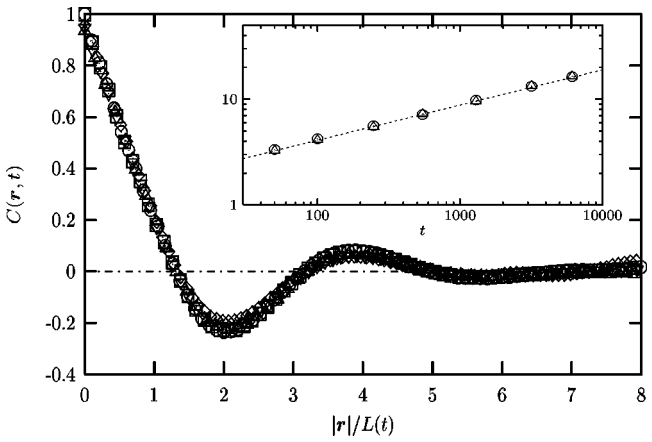

FIG. 3. Main figure: Circularly averaged two-point correlation as a function of the rescaled variable $|\mathbf{r}|/L(t)$ for different times in the range [50,1000]. By construction, one has $C(L(t),t)=0.2$, and the choice of 0.2 is indifferent. Inset: Growth laws in the x (circles) and y (triangles) directions. The dashed line is a fit to a power law $t^{1/3}$.

initial transient, so that large domains will have already grown. Such initial conditions are discussed at the end of the paper.

III. ZERO SHEAR CASE

Although the $\gamma=0$ case was extensively studied [1–3], we briefly consider this well-known situation with three aims. These results are presented to (i) validate our numerical procedure, (ii) present the quantities of interest, and, above all, (iii) make comparisons to the sheared case easier.

The domain growth typically takes place as in Fig. 1, where an isotropic bicontinuous structure coarsens with time. This coarsening process is well characterized by a two-point correlation function defined by

$$C(\mathbf{r},t)\equiv\frac{1}{V}\int d^2\mathbf{x}\langle\phi(\mathbf{x},t)\phi(\mathbf{x}+\mathbf{r},t)\rangle, \tag{6}$$

which is nothing but the Fourier transform of the structure factor, experimentally measured through light scattering experiments. A typical two-point function is represented in Fig. 2, which shows the isotropy of this surface. The average shape of the domains of Fig. 1 may be extracted from this plot by taking the intersection of this surface with a horizontal plane $z=$const. This allows us to measure the time dependence of the length scale $R_x(t)$ [respectively $R_y(t)$] in a direction x (respectively y). Both length scales are represented in the inset of Fig. 3, and have the expected power law behavior $R_x\simeq R_y\propto t^{1/3}$ [1–3].

The dynamic scaling hypothesis is tested in the main frame of Fig. 3, where the two-point function is circularly averaged and plotted as a function of $|\mathbf{r}|/L(t)$. This works perfectly well. We are thus confident in our numerical setup, and we shall now address the question of the influence of the shear flow on the spinodal decomposition.

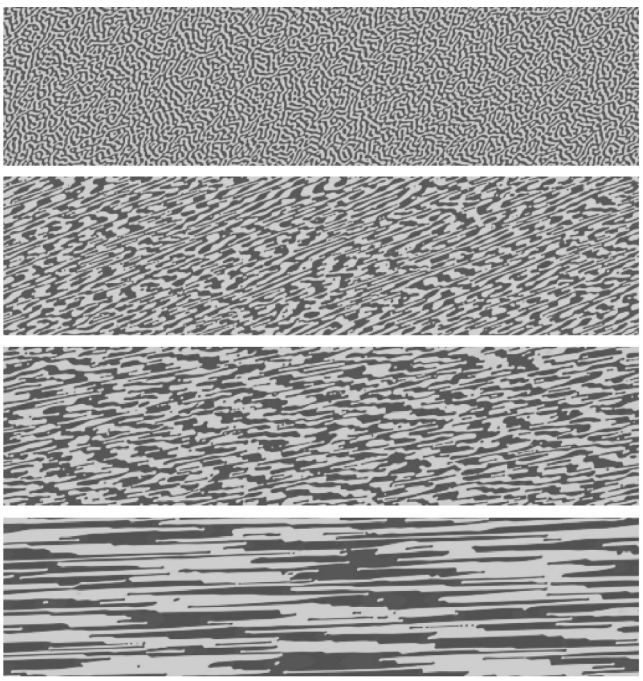

FIG. 4. Snapshots of sizes $L_y=512$ and $L_x=2048$ (parts of a 512×4096 system) for a shear rate $\gamma=0.01$, and strains $S(t)=1$, 5, 10, and 50 (from top to bottom). Each color represents one phase of the mixture.

IV. ANISOTROPIC GROWTH OF THE DOMAINS UNDER SHEAR

A. Basic observations

The time evolution of the domains when a shear flow is applied is followed in Fig 4. This evolution is the basic result of all previous numerical works [12–23], and shows that the domain growth is essentially unaffected for times $t\lesssim\gamma^{-1}$, since the first snapshot is very similar to those in Fig. 1. At intermediate times, the domains begin to have an anisotropic shape: the average direction of the domains is clearly apparent. This direction rotates and becomes more aligned with the flow when the strain increases. At large times $t\gg\gamma^{-1}$, domains are nearly aligned with the flow, and have a strongly anisotropic shape.

These features are also clearly discernible in Fig. 5, where

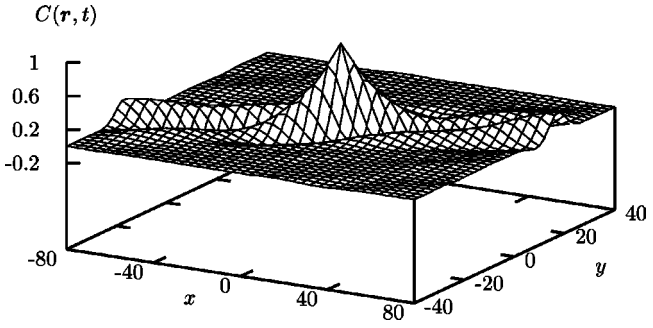

FIG. 5. Two-point correlation function for $\gamma=0.01$ and $S(t)=5$. The surface is stretched in the x direction. Note, in particular, that the x and y ranges are different in this figure.

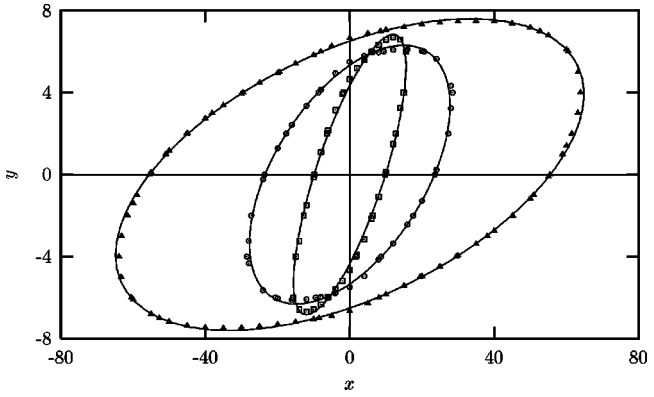

FIG. 6. Time evolution of the intersection of the two-point correlation with a horizontal plane, for strains $S(t)=5$ (squares), 10 (circles), and 20 (triangles), and a shear rate $\gamma=0.01$. The points are the data, while the lines are fits to an elliptic shape. Note, in particular, that the x and y ranges are different in this figure.

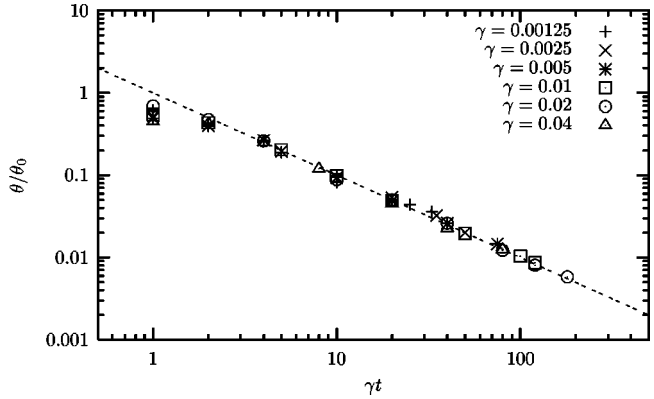

FIG. 7. Mean orientation of the domains as a function of the strain $S(t)=\gamma t$. The straight line is $1/\gamma t$.

we plot the two-point correlation function for a strain $S(t)=5$ at $\gamma=0.01$. The surface is clearly stretched in the flow direction (compare with Fig. 2). In particular, it becomes impossible to perform a circular average as in the unsheared case: isotropy is lost.

The average shape of the domains is again recorded through the intersection of the two-point correlation function with a horizontal plane. For definiteness, we take $z=0.5$, but the value 0.5 is unimportant. It is found numerically that this intersection is very well represented by an ellipse. Computing the parameters of this ellipse then gives access to two typical length scales, $R_{\|}(t)$ (large axis) and $R_{\perp}(t)$ (small axis), and to the mean orientation of the domains, $\theta(t)$ (the angle between the large axis and the x direction). We present the typical time evolution of the elliptic shape of the domains in Fig. 6, where data are also fitted to an elliptic form in a very satisfactory way. These three quantities depend both on the time t and on the shear rate γ, and in the following subsections we successively study the time evolution of $\theta(t)$ and the length scales $R_{\|}(t)$ and $R_{\perp}(t)$.

Before performing this analysis, a remark has to be made about the identification of the relevant length scales. It is quite clear from the above analysis that three parameters are needed to fully characterize the growing structure under shear. This feature was already noted in experiments [5,6]. In some of the previous numerical works, only two parameters were studied, namely, length scales in the x and y directions. Although these length scales should well represent the structure at long times, it is instead physically preferable to study the domain size in the directions defined by the angle $\theta(t)$. In Ref. [15], the direction of the domains' shape was recorded, but there was no attempt at a quantitative analysis of its behavior. We note, finally, that this quantitative analysis of the domain morphology in two dimensions naturally arises from the analytical work of Ref. [25], in the case of a nonconserved order parameter.

B. Mean orientation θ(t)

The first effect of the shear flow is to give the domains an anisotropic shape, and hence to create a preferred direction in the system. Physically, it can be expected that for a given shear rate γ, the mean orientation of the domains is inversely proportional to the strain $S(t)$, as would be the case for a rigid rod advected by the shear flow:

$$\theta(t)\simeq\frac{\theta_0(\gamma)}{\gamma t}. \tag{7}$$

This relation is tested in Fig. 7, where $\theta_0(\gamma)$ is used as an adjustable parameter. This figure shows that relation (7) is well satisfied in the whole range of shear rates investigated.

The parameter θ_0 is found to be a slowly increasing function of the shear rate. One finds $\theta_0(0.00125)\simeq 0.975$ and $\theta_0(0.04)\simeq 2.0$. By definition, this angle corresponds to the mean orientation of the domains when the strain is 1, $\theta_0\equiv\theta(t=\gamma^{-1})$, and its variation may be understood by the following argument. For times $t\leqslant\gamma^{-1}$, the domain growth is mainly unaffected by the flow, and thus, the larger the shear rate, the smaller the domains at time $t\sim\gamma^{-1}$. Since large domains are more easily deformed than small ones (because of the surface tension), it is expected that, at strain $S(t)\sim 1$, large domains (small γ) are more deformed than small ones (large γ). Hence, the smaller the shear rate, the smaller θ_0.

C. Growth laws

We now turn to the time evolution of the two length scales $R_{\perp}(t)$ and $R_{\|}(t)$. These quantities are studied for a very broad range of shear rates from $\gamma=0.04$ ($\gamma^{-1}=25$) to $\gamma=0.00125$ ($\gamma^{-1}=800$). All our results are summarized in Fig. 8, where $R_{\|}$ and $R_{\perp}$ are represented for each value of the shear rate as functions of the strain. We obtain numerically that the growth laws are well represented at large strains by the algebraic forms

$$R_{\|}(t)\simeq R_{\|0}(\gamma t)^{\alpha_{\|}},\quad R_{\perp}(t)\simeq R_{\perp 0}(\gamma t)^{\alpha_{\perp}}, \tag{8}$$

which define the growth exponents $\alpha_{\|}$ and $\alpha_{\perp}$. This was first obtained in a simulation by Padilla and Toxvaerd [22] and subsequently in similar systems in Refs. [9,12,18,25].

In Fig. 8, we fit our data using forms (8). These fits deserve some comments. The growth law for $R_{\|}$ becomes a nice straight line in a log-log plot at large strains $S(t)\gtrsim 10$.

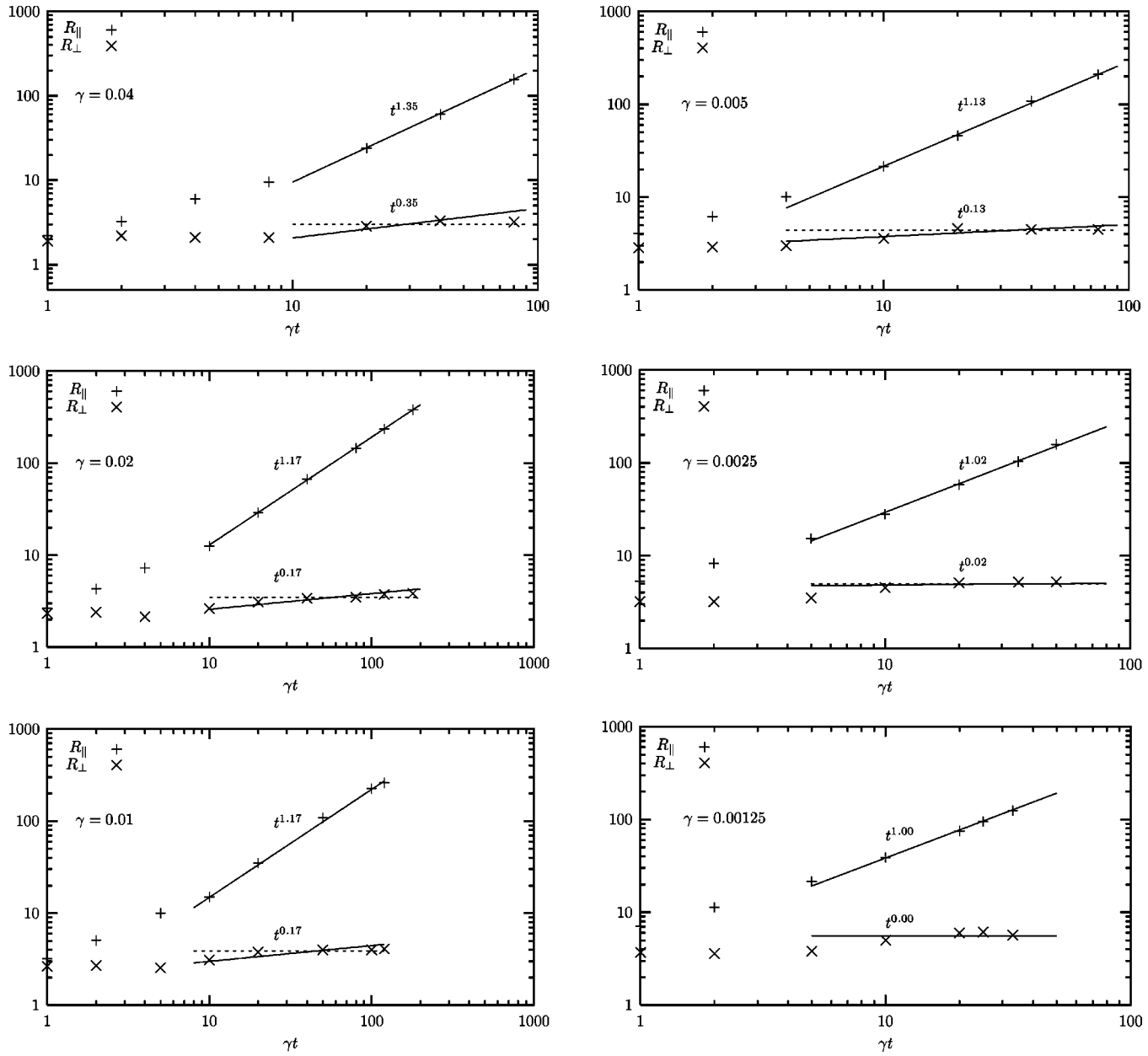

FIG. 8. The two length scales $R_\perp(t)$ and $R_\parallel(t)$ are represented as functions of the strain. Each figure is labeled by the corresponding shear rate. The symbols are the data, and the full lines are algebraic fits with the exponents indicated near each fit. For the strongest shear rates, a horizontal dashed line has been added as a fit to $\alpha_\perp = 0$.

Only the data points for such large strains are used to compute the exponent $\alpha_\parallel$. Concerning the time behavior of $R_\perp(t)$, two different fits were tested. First, a horizontal line corresponding to $\alpha_\perp = 0$ was compared to the data. Second, following the available analytical results [12,24,25], we also tried to fit the data with the ansatz

$$\alpha_\perp = \alpha_\parallel - 1. \tag{9}$$

Note that both fits are equivalent when $\alpha_\parallel = 1$, which is nearly the case for the two smallest shear rates. Several comments are in order.

(1) The algebraic fits are clearly a very good representation of the data. Some logarithmic corrections that come from an analytical study of the $O(n)$ model and of the nonconserved case may be present, but we do not expect to be able to determine them numerically.

(2) Although relation (9) reasonably accounts for the data, the value $\alpha_\perp = 0$ is also possible, and works well for *all* the shear rates investigated. This means that it could be possible to rescale all the curves for $R_\perp(t)$ by plotting $R_\perp(t)/R_{\perp 0}$ as a function of the strain for different shear rates, using $R_{\perp 0}$ as a fitting parameter. This parameter is found to be a decreasing function of the shear rate, which means that the smaller the shear rate, the wider the domains. This rescaling is performed in Fig. 9, and the data are indeed compatible with this hypothesis. Let us add the remark that $R_\perp(t)$ varies (at most) by a factor 2 in all the simulations. This strongly sup-

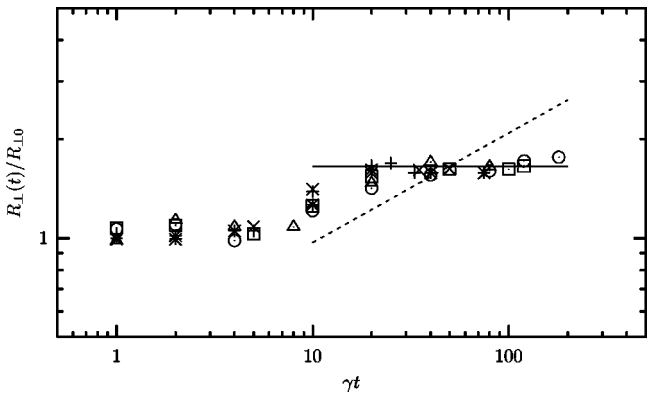

FIG. 9. Test of relation (8) for the small axis of the ellipse. The full line represents the case $\alpha_\perp = 0$, whereas the dashed line is for $\alpha_\perp = 1/3$. The symbols are the same as in Fig. 7. The latter exponent is clearly inconsistent with the numerical measurements for all the shear rates.

ports the hypothesis that there is in fact no growth in the perpendicular direction. Of course, once again, logarithmic corrections cannot be numerically dismissed.

(3) We do not see any evidence of the oscillations reported in Refs. [12,18]. We do not have a clear explanation for this, but a hypothesis is that these oscillations are a preasymptotic artifact of the measure process itself. The definition of the length scales used in Ref. [12] leads in some cases to a ratio $R_x(t)/R_y(t) \simeq 10$ for a strain $S(t) \simeq 1$ [12]. For this strain, the domains are still nearly circular; in our simulations, this ratio is never above the value 1.5. However, this argument is made weaker by the observation that Qiu *et al.* [9] used the same measurement procedure as Corberi *et al.* [12] at a lower shear rate $\gamma = 0.01$, and did not observe any oscillations.

(4) An important point is the fact that the exponents apparently depend on the value of the shear rate. More precisely, we find that $\alpha_\parallel$ decreases from a value of $\alpha_\parallel \simeq 1.35$ at $\gamma = 0.04$ to one of $\alpha_\parallel \simeq 1.0$ at $\gamma = 0.00125$. This means that we are in fact measuring *effective exponents*, and that the true asymptotic behavior has not been reached in some of the cases studied here.

The problem is then to determine which exponent is the right one. As emphasized in Sec. I, well-defined interfaces exist only if $\gamma \ll 1$. This indicates that a ''true'' asymptotic behavior is reached for the smallest shear rates investigated, and favors the value $\alpha_\parallel = 1$ found for $\gamma = 0.0025$ and 0.00125. Together with the behavior of $\alpha_\perp$ and the observation that the domains are wider at lower shear rates, we are led to the conclusion that the growth exponents are given by

$$\alpha_\parallel = 1, \quad \alpha_\perp = 0. \tag{10}$$

The analysis of dynamic scaling properties in the following section will reinforce this conclusion.

V. DYNAMIC SCALING

The last question we wish to address is the problem of dynamic scaling. We recall in Fig. 3 (where $\gamma = 0$) that the two-point correlation function has the property that it can be rescaled in the form of a single variable function

$$C(\mathbf{r},t) = \mathcal{C}\left(\frac{|\mathbf{r}|}{L(t)} \right). \tag{11}$$

This indicates that $L(t)$ is the only relevant length scale in the asymptotic regime characterized by $\xi \ll L(t)$. This behavior is the basis for a scaling argument which, in the unsheared case, allows an elegant derivation of the growth laws [30].

In the shear flow, there are two relevant length scales, and the scaling [Eq. (11)] can thus no longer be true. Two different generalizations were suggested by analytical works. The solution of the $O(n)$ model predicts the scaling form [24]

$$C(\mathbf{r},t) = \mathcal{C}\left(\frac{x}{R_x(t)}, \frac{y}{R_y(t)} \right), \tag{12}$$

where R_x and R_y are typical sizes in the directions x and y, respectively. A different scaling is expected from the nonconserved order parameter case, namely [25],

$$C(\mathbf{r},t) = \mathcal{C}\left(\frac{r_\parallel}{R_\parallel(t)}, \frac{r_\perp}{R_\perp(t)} \right), \tag{13}$$

where the subscripts refer to the rotating frame described previously. Corberi *et al.* [12] used the form of Eq. (12) as a starting point to generalize the argument of Bray [30] to the sheared case. It is thus important to see if this scaling behavior is detected in the simulation. Let us note that the tilt angle $\theta(t)$ is very small in the long time regime we are interested in. Then, one might ask if the difference between the forms of Eqs. (12) and (13) proposed above is relevant. Since the domains are very elongated in the x direction, then even with a small angle there might be differences between the ''parallel'' and x directions. Concerning y and ''perpendicular'' directions, the support of the correlation function in these directions is very small, so that differences between the two are indeed not observable.

We now present our numerical results. In Fig. 10, for two different shear rates we show an attempt at a rescaling of the two-point function in the x direction. In each case, we consider a time window where a hypothetical scaling might hold [i.e., the growth law reaches its algebraic asymptotic form, $S(t) \gtrsim 10$]. We also choose $R_x(t)$ in order to obtain the best collapse of the data. Clearly, the scaling [Eq. (12)] does not work in cases of either a high or a low shear rate.

In Fig. 11 we investigate the possibility that the second scaling form will hold in a direction defined by the tilt angle $\theta(t)$. Here there is a clear qualitative difference between the shear rates $\gamma = 0.0025$ and 0.04; the collapse of the data is excellent for the small shear rate, whereas there is a clear systematic evolution for the highest shear rate.

In our opinion, these results are a very good indication that the scaling form [Eq. (12)] does not describe the asymptotic behavior of the Cahn-Hilliard equation. Moreover, they show that a self-similar asymptotic regime has

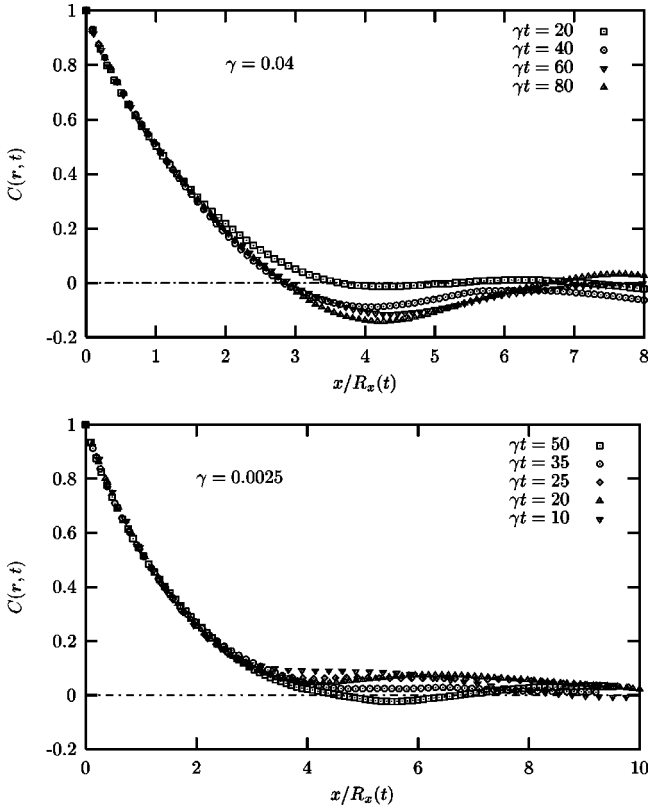

FIG. 10. Test of the dynamic scaling in the x direction for $\gamma=0.04$ and 0.0025. In both cases, the collapse is not satisfactory.

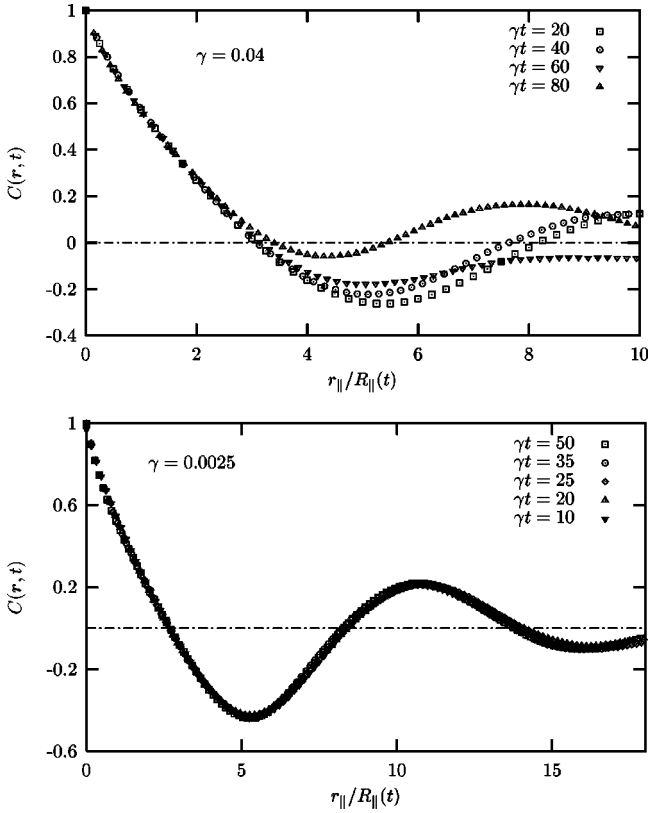

FIG. 11. Test of the dynamic scaling in the ''parallel'' direction for $\gamma=0.04$ and 0.0025. The collapse is very good for 0.0025 only, while there is a systematic evolution for 0.04.

been reached for the lowest shear rates investigated, characterized by the scaling [Eq. (13)] of the two-point function.

This is also confirmed by an inspection of the scaling properties in the parallel direction (which is equivalent to the y direction). In Fig. 12, we show the results for this direction. Once again, the collapse is very good for the low shear rate $\gamma=0.0025$, whereas it is clearly not satisfying for a higher shear rate $\gamma=0.04$.

VI. DISCUSSION

In this paper we have investigated the ordering kinetics of a binary mixture quenched below its spinodal line in a homogeneous shear flow, through a numerical solution of the Cahn-Hilliard equation in two spatial dimensions.

We have found that the bicontinuous coarsening structure is well described by three parameters. Since the average shape of the domains is elliptic, it is sufficient to give the lengths $R_\perp(t)$ and $R_\parallel(t)$ of the two principal axis of the ellipse, and the orientation of the large axis with respect to the flow, $\theta(t)$. We have measured the time evolution of these three quantities, defined from the two-point correlation function, and all our results may be summarized by the following relations, which have been shown to hold in the asymptotic regime of large times:

$$R_\parallel(t) \simeq \gamma t,$$

$$R_\perp(t) \simeq \text{const},$$

$$\theta(t) \simeq \frac{1}{\gamma t},$$

$$C(\mathbf{r},t) \simeq \mathcal{C}\left(\frac{r_\parallel}{R_\parallel(t)}, \frac{r_\perp}{R_\perp(t)}\right). \tag{14}$$

In particular, this asymptotic regime could not be reached for the largest shear rates we have investigated. Moreover, our attempts at detecting (in the cases $\gamma=0.04$ and 0.02) a crossover from a preasymptotic regime with $\alpha_\parallel>1$ and $\alpha_\perp>0$ toward regime (14) were unsuccessful, because this would require too large a system size L_x. These results also demonstrate that the domain growth does not stop under the shear flow, in the case where hydrodynamics is neglected and answer then questions (1)–(4) of Sec. I.

We now compare our results with previous ones. It is interesting to note that, even though this simulation was not intended to be able to reproduce experiments since hydrodynamics has been neglected, our results quantitatively reproduce the experiments of Chan *et al.* [6,11] on a mixture of water and isobutyric acid, and those of Qiu *et al.* [21] on a polymer blend of polystyrene and poly-(vinyl methyl ether), for the three quantities describing the morphology of the domains. These experiments were probably done in a regime where hydrodynamic effects are negligible, since other experiments by Hashimoto and co-workers [7] reported a saturation of the domains to a γ-dependent size. This stationary

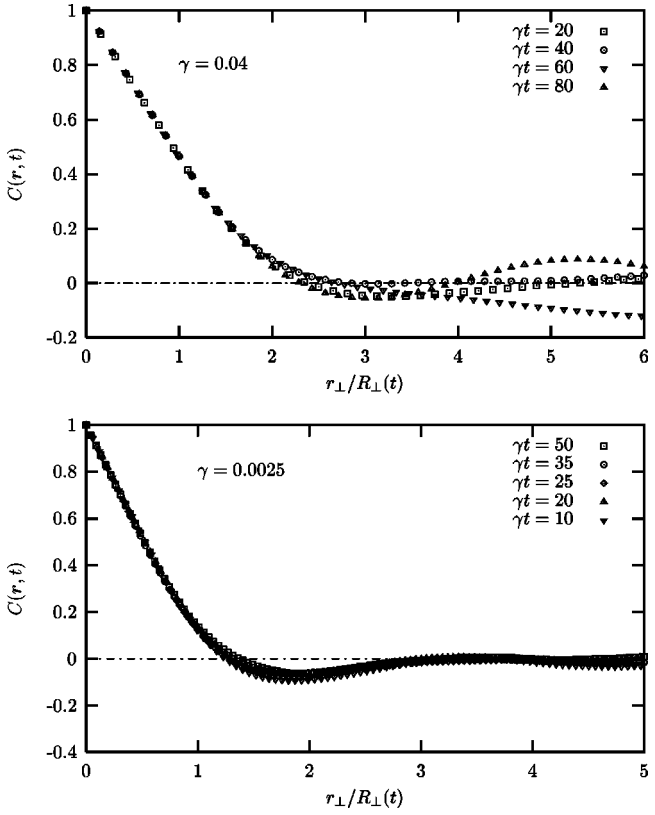

FIG. 12. Test of the dynamic scaling in the parallel (or equivalently y) direction for $\gamma = 0.04$ and 0.0025. The collapse is very good for the lowest shear rate.

steady state has been termed a ''string phase,'' and was also observed by Hobbie *et al.* [8] in a strong shear rate regime.

Our numerical findings can be compared with previous works neglecting hydrodynamics, and our results for the growth laws are similar to those found by Qiu *et al.* [21] and Corberi *et al.* [12]. Note that in this last reference [12], the growth laws were compatible with regime (14), although they are compared with the behaviors $R_x(t) \sim t^{4/3}$ and $R_y(t) \sim t^{1/3}$. However, the authors admitted that the latter regime was not reached within the numerical time window. Earlier simulations were not able to be very quantitative [19,20,22,23], although Padilla and Toxvaerd [22] suggested that the anisotropic domain growth was well described by algebraic laws. This is, to our knowledge, the first time that the elliptic average shape of the domains was systematically investigated in a numerical experiment. Concerning the scaling of the the two-point correlation function, Qiu *et al.* [21] showed that form (12) is not appropriate, but they did not investigate form (13).

Analytically, the known results in the case of a conserved order parameter are for the $O(n)$ model, which was solved with shear in the large-n limit [24] (also see Ref. [18]). The second result stems from a scaling argument developed by Corberi *et al.* [12]. Both predict that the growth laws should be $R_x(t) \sim t^{4/3}$ and $R_y(t) \sim t^{1/3}$, with a scaling form for $C(\mathbf{r},t)$ as in Eq. (12). Our results do not corroborate these predictions. A reason for this may be that these results do not take into account the elliptic shape of the domains, and we have clearly demonstrated this could be a key point in understanding the scaling properties of the system. One might also question the validity of a renormalization-group type argument in the case where the exponent $\alpha_\perp$ is zero, since, upon space rescaling, domains become thinner and thinner. Recently [25], an approximate solution of the case of a nonconserved order parameter was found, predicting the scaling [Eq. (13)] in two spatial dimensions. However, extending this solution to the conserved case is certainly a very hard task, since in the unsheared case the conservation law already makes the calculations very involved [3].

We are then faced with the problem of having numerical results that cannot be understood within an existing analytical framework. We now give a simple physical argument leading to Eqs. (14), inspired by the original argument given by Huse [31] to describe the zero-shear case. The spinodal decomposition under a shear flow results basically from two competing effects.

(i) The advection of the order parameter, which becomes efficient for times $t \gtrsim \gamma^{-1}$, deforms the nearly circular domains existing at time $t \sim \gamma^{-1}$. It is very easy to compute that, with advection only, a circular domain is deformed into an elliptic shape with principal axes scaling at large strain as $R_\perp(t) \sim (\gamma t)^{-1}$ and $R_\parallel(t) \sim \gamma t$, with a tilt angle $\theta(t) \sim (\gamma t)^{-1}$.

(ii) The domain growth arises because of the existence of a gradient of the chemical potential $\mu \equiv \delta F / \delta \phi$. This force gives rise to currents which make an interface of curvature R move with a velocity $dR/dt \propto 1/R^2$. This interface motion results, in the absence of shear, to a coarsening of the domain structure [31]. Here we modify this argument by taking into account the fact that the structure is no longer isotropic. While the domain growth does not affect the tilt angle $\theta(t)$, it leads to two different interface velocities, namely, $dR_\parallel/dt \sim -1/R_\perp^2$ and $dR_\perp/dt \sim +1/R_\parallel^2$.

With the strong assumption that a balance can be made between these two effects, this leads to the following equations for the the three parameters of the ellipse:

$$\frac{dR_\perp(t)}{dt} = -\frac{1}{\gamma t^2} + \frac{1}{R_\parallel(t)^2}, \tag{15}$$

$$\frac{dR_\parallel(t)}{dt} = +\gamma - \frac{1}{R_\perp(t)^2}, \tag{16}$$

$$\theta(t) = \frac{1}{\gamma t}, \tag{17}$$

which indeed imply Eqs. (14). Although simple and heuristic, this argument in fact captures the essence of the coarsening process under a shear flow. It should correctly describe the domain growth when the domains are quite large. Otherwise, the notion of interface velocity is meaningless. However, it is quite clear that subtleties, such as logarithmic corrections that exist in more involved computations [25], will not be captured by such a naive argument.

Let us note that when it is applied to the nonconserved case, this argument leads to the growth laws $R_\perp \sim$ const and

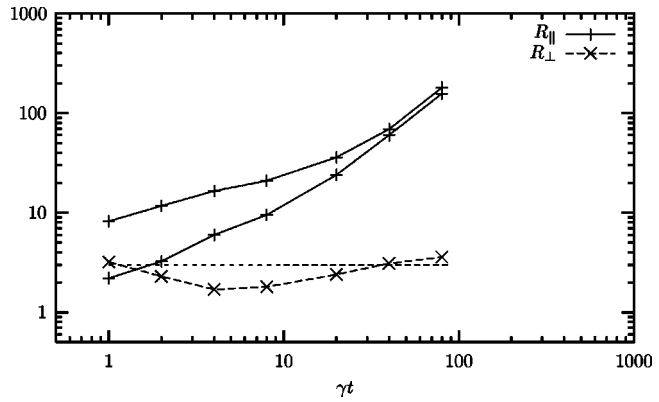

FIG. 13. Time evolution of the two length scales as a function of the strain when the system is first allowed to grow without shear during a time $t=400$, and then submitted to a shear flow with $\gamma=0.04$. As a visual guide we have added a horizontal dashed line, and the data for $R_\parallel(t)$ for a direct quench in the shear flow (lowest $R_\parallel$ curve).

$R_\parallel \sim t$, at leading order. This not so far from the results $R_\perp \sim (\ln t)^{-1/4}$ and $R_\parallel \sim t(\ln t)^{1/4}$ found in Ref. [25].

The second point we want to note is that these equations may be used to understand the following experiment. We mentioned above the possibility of applying the shear flow at a certain time after the quench, in order to have large circular domains as initial conditions. From Eqs. (15)–(17), we expect the following behavior. For a relatively small strain, since the domains are quite large, the second term on the right-hand side of Eq. (15) is negligible, and $R_\perp$ first *decreases*. Thus the second term on the right-hand side of Eq. (16) becomes important and the growth of $R_\parallel$ is slower than for a direct quench in the flow. This initial behavior is qualitatively different from the previous case, and after this unusual transient the growth becomes similar to the growth studied previously. This predicted behavior agrees satisfactorily with the corresponding numerical experiment, as can be seen in Fig. 13. Note, in particular, that the slope of the curve $R_\parallel(t)$ is minimum when $R_\perp(t)$ reaches its smallest value, as can also be deduced from Eq. (16).

In conclusion, we hope this work has clarified several issues concerning spinodal decomposition in a shear flow. It would be very interesting to perform the same measurements in three dimensions, since the analytical approach of Ref. [25] shows that dynamic scaling properties might be different in two and three dimensions. Of course, the next (big) problem is to have a better understanding of the effect of hydrodynamics on the phase separation in a shear flow.

ACKNOWLEDGMENTS

This work was supported by the Pôle Scientifique de Modélisation Numérique at École Normale Supérieure de Lyon. It was motivated by the constant interest and encouragements shown by A. J. Bray, and I wish to thank him warmly for his support. I also sincerely thank A. Cavagna for his numerous interesting comments and questions on this work. I am grateful to J.-L. Barrat and J. Kurchan for the continuous and fruitful interactions we had over the last two years.

[1] P. C. Hohenberg and B. I. Halperin, Rev. Mod. Phys. **49**, 435 (1977).
[2] J. D. Gunton, M. San Miguel, and P. S. Sathni, in *Phase Transitions and Critical Phenomena*, edited by C. Domb and J. L. Lebowitz (Academic Press, New York, 1988), Vol. 8.
[3] A. J. Bray, Adv. Phys. **43**, 357 (1994).
[4] A. Onuki, J. Phys.: Condens. Matter **9**, 6119 (1997), and references therein.
[5] D. Beysens, M. Gbadamassi, and B. Moncef-Bouanz, Phys. Rev. A **28**, 2491 (1983).
[6] C. K. Chan, F. Perrot, and D. Beysens, Phys. Rev. Lett. **61**, 412 (1988).
[7] T. Hashimoto, K. Matsuzaka, E. Moses, and A. Onuki, Phys. Rev. Lett. **74**, 126 (1995); K. Matsuzaka, T. Koga, and T. Hashimoto, *ibid.* **80**, 5441 (1998).
[8] E. K. Hobbie, S. Kim, and C. C. Han, Phys. Rev. E **54**, R5909 (1996).
[9] F. Qiu, J. Ding, and Y. Yang, Phys. Rev. E **58**, R1230 (1998).
[10] J. Läuger, C. Laubner, and W. Gronski, Phys. Rev. Lett. **75**, 3576 (1995).
[11] C. K. Chan, F. Perrot, and D. Beysens, Phys. Rev. A **43**, 1826 (1991).
[12] F. Corberi, G. Gonnella, and A. Lamura, Phys. Rev. Lett. **83**, 4057 (1999); the three-dimensional case was considered by F. Corberi, G. Gonnella, and A. Lamura, e-print cond-mat/0009168.
[13] M. E. Cates, V. M. Kendon, P. Bladon, and J.-C. Desplat, Faraday Discuss. Chem. Soc. **112**, 1 (1999).
[14] Z. Shou and A. Chakrabarti, Phys. Rev. E **61**, R2200 (2000).
[15] A. J. Wagner and J. M. Yeomans, Phys. Rev. E **59**, 4366 (1999).
[16] Z. Zhang, H. Zhang, and Y. Yang, J. Chem. Phys. **113**, 8348 (2000).
[17] R. Yamamoto and X. C. Zeng, Phys. Rev. E **59**, 3223 (1999).
[18] F. Corberi, G. Gonnella, and A. Lamura, Phys. Rev. Lett. **81**, 3852 (1998); Phys. Rev. E **61**, 6621 (2000).
[19] D. H. Rothman, Phys. Rev. Lett. **65**, 3305 (1990); Europhys. Lett. **14**, 337 (1991).
[20] C. K. Chan and L. Lin, Europhys. Lett. **11**, 13 (1990).
[21] F. Qiu, H. Zhang, and Y. Yang, J. Chem. Phys. **108**, 9529 (1998).
[22] P. Padilla and S. Toxvaerd, J. Chem. Phys. **106**, 2342 (1997).
[23] T. Ohta, H. Nozaki, and M. Doi, J. Chem. Phys. **93**, 2664 (1990).
[24] N. P. Rapapa and A. J. Bray, Phys. Rev. Lett. **83**, 3856 (1999); N. P. Rapapa, Phys. Rev. E **61**, 247 (2000).
[25] A. J. Bray and A. Cavagna, J. Phys. A **33**, L305 (2000); A. Cavagna, A. J. Bray, and R. D. M. Travasso, Phys. Rev. E **62**, 4702 (2000).

[26] A. J. Bray, in *Soft and Fragile Matter, Nonequilibrium Dynamics, Metastability and Flow*, edited by M. E. Cates and M. R. Evans (Institute of Physics Publishing, Bristol, 2000).
[27] T. M. Rogers, K. R. Elder, and R. C. Desai, Phys. Rev. B **37**, 9638 (1988).
[28] A. Onuki, J. Phys. Soc. Jpn. **66**, 1836 (1997).
[29] L. Berthier, J.-L. Barrat, and J. Kurchan, Eur. Phys. J. B **11**, 635 (1999).
[30] A. J. Bray, Phys. Rev. B **41**, 6724 (1990).
[31] D. A. Huse, Phys. Rev. B **34**, 7845 (1986).